SINTEF
PROCEEDINGS 5

International Conference Organised by IBPSA-Nordic, 13th–14th October 2020, OsloMet

BuildSIM-Nordic 2020

Selected papers

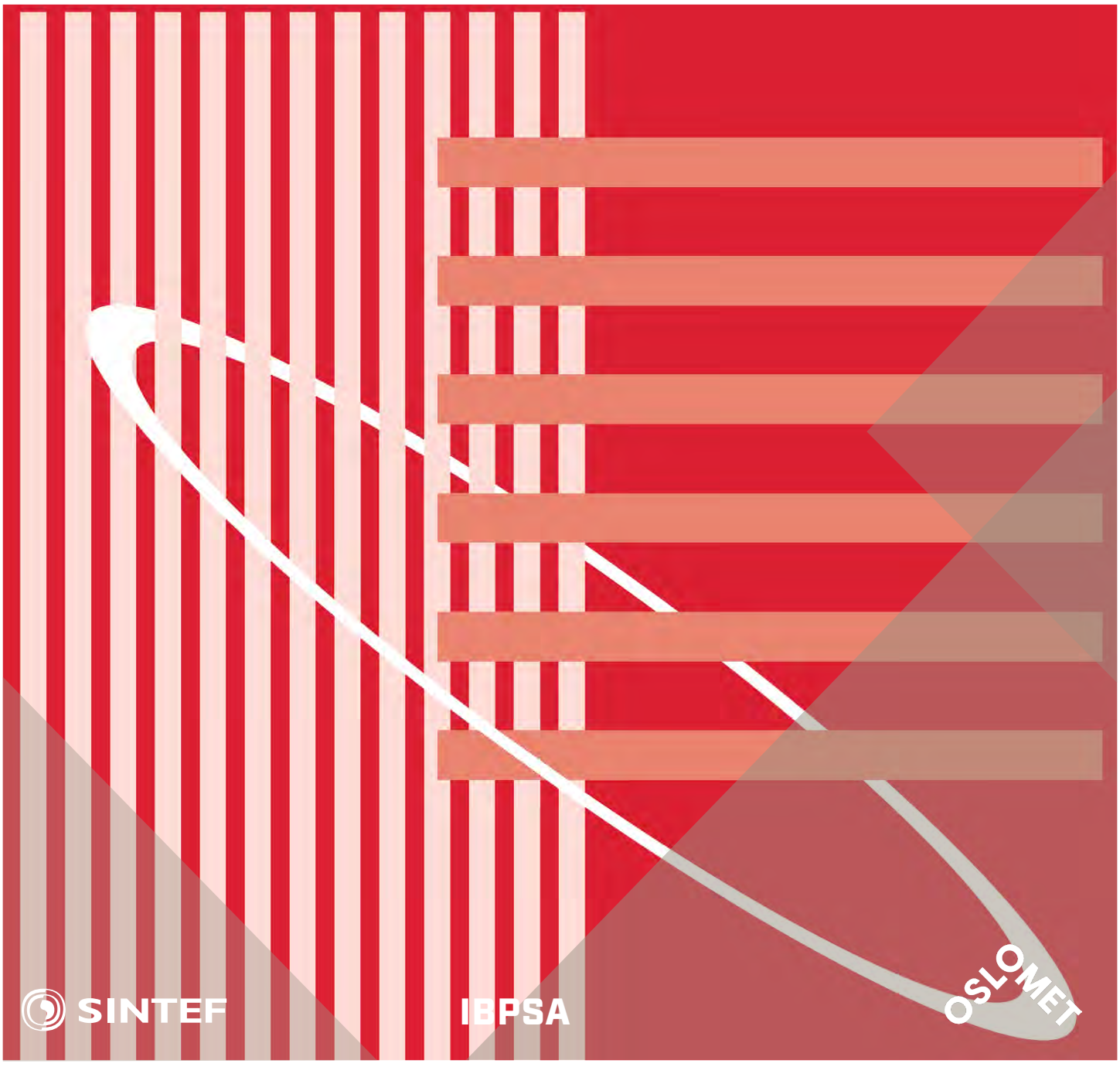

SINTEF Proceedings

Editors:
Laurent Georges, Matthias Haase, Vojislav Novakovic and Peter G. Schild

BuildSIM-Nordic 2020

Selected papers

International Conference Organised by IBPSA-Nordic,
13th–14th October 2020, OsloMet

SINTEF Academic Press

SINTEF Proceedings no 5
Editors:
Laurent Georges, Matthias Haase, Vojislav Novakovic and Peter G. Schild
BuildSIM-Nordic 2020
Selected papers
International Conference Organised by IBPSA-Nordic,
13th–14th October 2020, OsloMet

Keywords:
Building acoustics, Building Information Modelling (BIM), Building physics, CFD and air flow, Commissioning and control, Daylighting and lighting, Developments in simulation, Education in building performance simulation, Energy storage, Heating, Ventilation and Air Conditioning (HVAC), Human behavior in simulation, Indoor Environmental Quality (IEQ), New software developments, Optimization, Simulation at urban scale, Simulation to support regulations, Simulation vs reality, Solar energy systems, Validation, calibration and uncertainty, Weather data & Climate adaptation, Fenestration (windows & shading), Zero Energy Buildings (ZEB), Emissions and Life Cycle Analysis

Cover illustration: IBPSA-logo

ISSN 2387-4295 (online)
ISBN 978-82-536-1679-7 (pdf)

SINTEF Academic Press
Address: Børrestuveien 3
PO Box 124 Blindern
N-0314 OSLO
Tel: +47 40 00 51 00

www.sintef.no/community
www.sintefbok.no

POD-interpolation based prediction of indoor airflows

Mats Kluftødegård, Arnab Chaudhuri
Department of Civil Engineering and Energy Technology
OsloMet — Oslo Metropolitan University, Oslo, Norway.

Abstract

This work reports a proper orthogonal decomposition (POD)-interpolation based prediction of indoor airflows related to displacement ventilation. Steady-state computational fluid dynamics (CFD) solution snapshots with varying relevant non-dimensional number are used to estimate the dominant POD coefficients/modal amplitudes and POD modes. A cubic spline interpolation of the POD coefficients is used to compute the solution for desired value of the non-dimensional number of interests. The verification and validation of this data-driven procedure is performed considering a 2D mixed convection problem involving a horizontal channel with cavity heated from below for a range of Richardson numbers. On the other hand, CFD solutions for a standard displacement ventilation configuration is used to decompose the flow field variables in terms of Archimedes number dependent POD coefficients and associated space dependent POD bases. A detailed analysis of the CFD and POD-interpolated predicted flow-field variables for displacement ventilation cases, error estimates and the spatial structures of the POD modes are presented.

Introduction

Fundamentally, air flow, heat and mass transfer phenomena govern the indoor air quality, thermal comfort and energy usage in buildings. Air change rate, pollutant removal, heat removal, exposure and air distribution are the key features to assess the performance of a heating, ventilating and air-conditioning (HVAC) system. Ventilation systems can be classified into various types depending upon the concentration distribution, location of the air supply/exhaust device and the use of natural and mechanical forces (Cao et al. (2014)). For several decades, a substantial scientific research focus has prevailed achieving design of energy efficient, effective airflow distribution and thermal comfort in buildings.

Displacement ventilation (DV) is potentially a very good ventilation strategy among the other types of air distribution principles where the contaminant air is removed from the ceiling level of a room. The exhaust temperature is higher than the occupied zone and a fresh air being supplied at the floor level (Nielsen (1988), Davidson (1989), Nielsen (2000)). A well designed DV system can be energy efficient to regulate room temperature and air velocity for thermal comfort and good air quality utilising natural convection currents (Cehlin and Moshfegh (2010)). Several key parameters for such systems are ventilation rate, location of the air terminal device, type of the diffuser and the supply air temperature (Yuan et al. (1998), Nordtest (2003)). Nevertheless, a DV configuration involves complex flow physics like gravity current, radiation effect and thermal stratification. Challenging issues related to thermal characterisation including radiation effects, draft discomfort, etc. are investigated by several researchers (Li et al. (1992), Causone et al. (2010), Magnier et al. (2012), Gilani et al. (2016)). The recent studies with DV systems addresses interesting aspects considering e.g., severe odor problems in hospital environments (Choi et al. (2019)), adaptive climate building with heat source/smart windows (Javad and Navid (2019)) and highly polluted indoor environment with dense oil mist in a machining plant (Wei et al. (2020)). Optimal design and modeling aspects of DV systems in diverse contexts are therefore important active research areas for HVAC scientists and engineers.

Apart from the advanced experimental measurements, CFD is widely used as a reliable numerical tool to predict a wide range of ventilation problems with detailed spatio-temporal distributions of flow-field variables. In CFD, the governing non-linear coupled partial differential equations are solved with a suitable discretization and solution procedure. However, high-fidelity CFD-simulations for design and optimization is indeed costly both in terms of necessary computer resource and CPU time. In this regard, POD based interpolation can be used, exploiting the CFD results with varying one or many parameters (e.g. relevant non-dimensional numbers involved in the governing phenomena) of interest to produce desired predictions in an efficient and cost effective manner. For example, considering a set of steady-state CFD solutions as "snapshots" the dominant POD coefficients/modal amplitudes and POD modes have to be estimated first. These intern can be used with a suitable interpolation of the coefficients to generate desired solution(s) for particular values of the parameter(s) of interest without performing costly CFD simulations. Some of the previous studies used steady state CFD solutions as snapshots for POD e.g., in in-

door airflow application (Elhadidi and Khalifa (2005) and for coupling between CFD and lumped parameter flow network zonal (FNZ) models Khalifa et al. (2007)).

This work aims to predict complex flow physics for a DV configuration of indoor environments using CFD snapshots and POD-interpolation method. CFD results are generated using the commercial computer program StarCCM+. We solved 2D/3D compressible Navier-Stokes equation (without Boussinesq approximation) together with mass and energy equations. Additionally, two-equation turbulence models are employed to account turbulent flow cases. The paper is organized as follows. In section **Method**, we present the governing equations and the overall POD methodology. The validation cases are presented thereafter. Subsequently, the problem setup of the displacement ventilation is given. The flow analysis given in the section **Results and discussion**. Finally, the conclusions are drawn at the end.

Method

Governing equations

In this study, we solve the compressible steady Navier-Stokes equations together with the mass and the energy conservation equations. The general transport equation for any conserved property ($\rho\phi$) can be expressed as in the following standard form, $\boldsymbol{\nabla}\cdot\rho\phi\mathbf{v} = \boldsymbol{\nabla}\cdot\Gamma\boldsymbol{\nabla}\phi + S_\phi$. Here ρ is the fluid density, $\mathbf{v}$ is the velocity vector and Γ is the diffusion coefficient. The governing equation involves advection term in left hand side and the terms on the right hand side signify the diffusion term and the generation term respectively. The gravity source term in the momentum equations is treated directly without Boussinesq approximation. Formulation of RANS (Reynolds averaged Navier Stokes) system of equations considering two equation SST (Menter) $\kappa-\omega$ turbulence model is used for turbulent flow cases. The choice of SST $\kappa-\omega$ model is based on the findings of Gilani et al. (2016), where the authors reported the superiority of the SST $\kappa-\omega$ model and the standard $\kappa-\omega$ model in predicting thermal plume and thermal stratification in a DV setup. Constitutive relation of Newtonian fluid and equation of state ideal gas close the system of equations with appropriate boundary conditions. We used the finite volume method (FVM) based commercial computer program StarCCM+ to solve the above mentioned governing equations. Second order implicit segregated/coupled flow solvers equipped with Roe schemes for convection, hybrid Gauss least-squared gradient method based 2nd order schemes for diffusion and Venkatakrisnan limiter function are chosen. Algebraic Multi-Grid (AMG) techniques are also invoked with the setup mentioned above.

POD snapshot method

Proper orthogonal decomposition (POD) method can be realized in several forms such as Karhunen-Loève decomposition (KLD), principal component analysis (PCA), and singular value decomposition (SVD) having wide spectrum of applications in scientific and engineering field. The key dominant characteristics/features in a data set can be recognized by a POD technique via low-dimensional descriptions for multidimensional systems. Originally, POD was introduced in the framework of fluid mechanics applications in late sixties. This was followed by the "snapshot POD" methodology by Sirovich and Kirby (1987) and the procedure is essentially a simple data-driven procedure closely related to principal component analysis (PCA), one of the fundamental algorithm of applied statistics and machine learning (Brunton et al. (2020)). In this work, the steady-state CFD solutions "snapshots" are used to decompose a non-dimensional flow variable $\phi^*(\Pi,\vec{x})$, where Π is a governing non-dimensional number of the flow physics under consideration. The decomposition essentially leads to the determination of a finite number of POD coefficients, $a_k(\Pi)$ and space dependent POD modes, $\psi_k(\vec{x})$ as,

$$\phi^*(\Pi,\vec{x}) \approx \sum_{k=1}^{m} a_k(\Pi)\psi_k(\vec{x}). \tag{1}$$

where, m is the number of snapshots for set of values of $\Pi_i \in [\Pi_{min},\Pi_{max}]$, $\forall\ i = 1,\ldots,m$. Once, the desired POD coefficients and POD modes are available, a suitable interpolation can be used to construct the flow field variables for any intermediate Π_{int}. The POD-interpolated prediction can be given by

$$\phi^*(\Pi_{int},\vec{x}) \approx \sum_{k=1}^{N} a_k(\Pi_{int})\psi_k(\vec{x}). \tag{2}$$

where $N \leq m$. We used a cubic spline interpolation to estimate $a_k(\Pi_{int})$ from $a_k(\Pi_i)$'s.

A brief methodology to determine the POD coefficients and the POD modes is given below (see Meyer et al. (2007), Selimefendigil (2013) for detail). First, the m number of CFD solution of ϕ^* on n mesh points can be arranged in a data set matrix $\boldsymbol{\Phi}^* = [\boldsymbol{\phi}^{*1}\boldsymbol{\phi}^{*2}\ldots\boldsymbol{\phi}^{*m}]$ as,

$$\boldsymbol{\Phi}^* = \begin{bmatrix} \phi_1^{*1} & \phi_1^{*2} & \phi_1^{*3} & \cdots & \phi_1^{*m} \\ \phi_2^{*1} & \phi_2^{*2} & \phi_2^{*3} & \cdots & \phi_2^{*m} \\ \vdots & \vdots & \vdots & \vdots & \vdots \\ \phi_n^{*1} & \phi_n^{*2} & \phi_n^{*3} & \cdots & \phi_n^{*m} \end{bmatrix}. \tag{3}$$

Then the auto covariance matrix is created. This matrix represents the covariance of the value with it self at some point. Where covariance is a measure

of the linear dependency of two values. This can be defined as:

$$\mathbf{C} = \frac{1}{m}\mathbf{\Phi}^{*\intercal}\mathbf{\Phi}^{*}. \tag{4}$$

The following eigenvalue problem then has to be solved:

$$\mathbf{C}\mathbf{X}^{i} = \lambda^{i}\mathbf{X}^{i}, \quad i = 1, 2, ..., m. \tag{5}$$

Where $\mathbf{X}$ is the eigenvector, and λ is the eigenvalues. This eigenvalue problem was solved using SVD. The solutions are ordered according to the size of the eigenvalues from highest to lowest. The eigenvectors, $\mathbf{X}^{i}$, in equation (5) forms a basis for making the POD modes, $\boldsymbol{\psi}^{i}$:

$$\boldsymbol{\psi}^{i} = \frac{\sum_{j=1}^{m} X_j^i \boldsymbol{\phi}^{*j}}{\left\| \sum_{j=1}^{m} X_j^i \boldsymbol{\phi}^{*j} \right\|}, \quad i = 1, 2, ..., m. \tag{6}$$

Where X_j^i is the j'th component of the eigenvector corresponding to the eigenvalue λ^i, and $\|\cdot\|$ is the second norm of any vector $\boldsymbol{\xi}$, given as:

$$\|\boldsymbol{\xi}\| = \sqrt{(\xi_1)^2 + (\xi_2)^2 + ... + (\xi_n)^2} \tag{7}$$

The POD coefficient can be determined by projecting $\boldsymbol{\phi}^{*m}$ onto the POD modes:

$$\mathbf{a}^{m} = \mathbf{\Psi}\boldsymbol{\phi}^{*m} \tag{8}$$

Where $\mathbf{\Psi} = [\boldsymbol{\psi}^1\boldsymbol{\psi}^2 \ldots \boldsymbol{\psi}^m]$ The snapshot $\boldsymbol{\phi}^{*m}$ can then be reconstructed by:

$$\boldsymbol{\phi}^{*m} = \mathbf{\Psi}^{\intercal}\mathbf{a}^{m} \tag{9}$$

The above methodology has been implemented via Python programming scripts and the data visualisation is performed by MATLAB programming scripts.

Validation

We first solved a 2D benchmark test case of laminar compressible flow through a horizontal channel with an open rectangular cavity in which a discrete hot surface is placed at the bottom wall of the cavity. The setup of this case is similar to that presented in Aminossadati and Ghasemi (2009) as well as in Selimefendigil (2013). The choice of this test case is very much relevant with respect to the indoor ventilation flow physics involving both heat transfer and fluid flow with the active gravity source term. A suitable 2D computational domain consisting of 5175 computational cells is used to simulate a case with Richardson number $Ri = 100$ where, $Ri = \dfrac{g\beta(T_h - T_c)L}{u_{in}^2}$. Here, g is the acceleration due to gravity, β is thermal expansion coefficient, T_h is the temperature of the hot surface, T_c is the temperature at the inlet, L is the characteristic length (depth of the cavity) and u_{in} is the inlet velocity. Laminar compressible segregated flow solver setup as mentioned before is used for CFD predictions. Converged solution is extracted once the residuals for all equations drops below 10^{-7}. Figure 1 shows a very good agreement of the present solution with the previous studies reported by Aminossadati and Ghasemi (2009) as well as Selimefendigil (2013) using Boussinesq approximation.

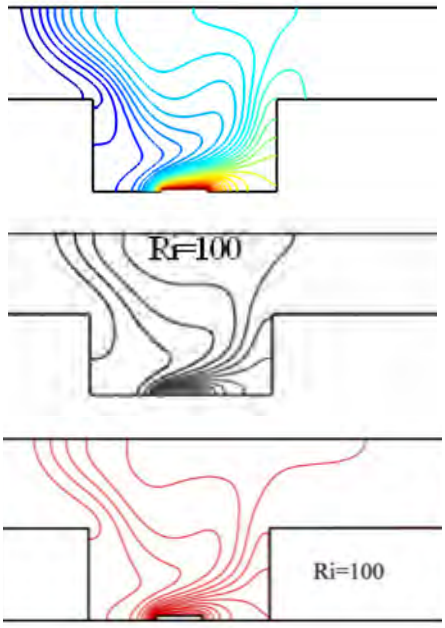

Figure 1: Comparison of numerical solutions, temperature contours for $Ri = 100$. top: present study, middle: Selimefendigil (2013), bottom: Aminossadati and Ghasemi (2009).

To verify the implementation of the overall POD methodology, steady state CFD solutions are performed with varying Ri, for a fixed value of Grashof number $Gr = 10^4$. The eight CFD solutions obtained via the same aforementioned convergence criteria for $Ri = 40, 50, 60, 70, 80, 90, 100$ and 110 are used as snapshots input data for the POD technique. Evidently with the increase of Ri the naturaal convection effects becomes dominant. The POD-interpolated solution for $Ri = 75$ is constructed and compared with the actual CFD solution for verification and validation. The contours of the non-dimensional temperature $\theta(Ri, \vec{x}) = (T - T_c)/(T_h - T_c)$ and the absolute error estimates (see Figure 2) clearly shows the reliability of the implementation. The spatial structures of the POD modes are shown in Figure 3. The relative energy of the POD modes can be estimated from the eigenvalues as $E_r = \lambda^i / \sum_{i=1}^{m} \lambda^i$. The energy associated with the first POD mode is found to be 99.99999% and the rest of the modes assume values of the order of 10^{-7}% or less. This reveals that the most of the energy contained within the first POD mode.

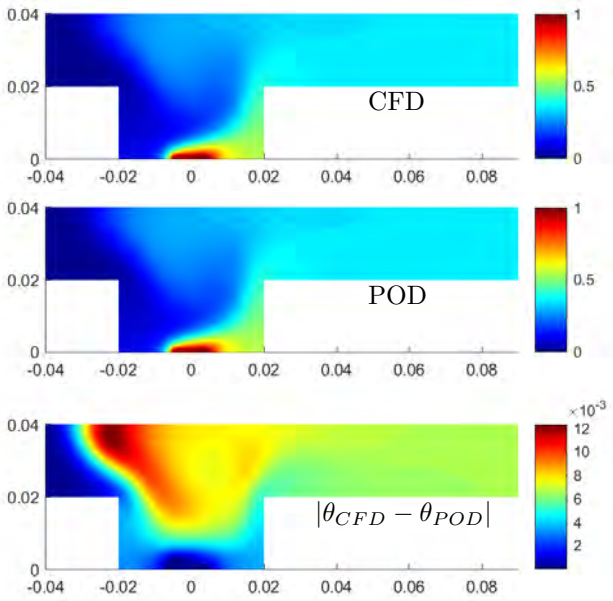

Figure 2: Comparison of CFD and POD predictions, contours of θ and error estimates for Ri=75.

Problem setup

In a DV system, the contaminated hot air from a room is displaced through ceiling level with fresh cold air supply at or near the floor level with a low velocity (typically < 0.5 m/s). This, usually create vertical gradients of air velocity, temperature and contaminant concentration (Cao et al. (2014)). The characteristics of the flow field depends on the type of air terminal device (DV unit) and the distribution of heat sources. To study the indoor airflows in DV configuration, a 3D computational domain of 7.5m(length) by 5.6m(width) by 2.8m(height) is taken (see Figure 4) as a standard room. The dimensions and the overall ventilation strategy with air supply diffuser and exhaust are set essentially following the guideline of the Nordtest method (Nordtest (2003)). A wall mounted displacement ventilation diffuser is placed at the floor level with an area of $0.24m^2$ having height, $h = 0.3m$. The air exhaust is placed on the opposite wall of the diffuser having the same dimensions. The heat loads are provided by heating wire around the room walls except the wall with the air supply. This is placed at $0.7m$ above the floor with a thickness of $0.05m$. Figure 4 also shows the mesh arrangements within the computational domain. Surface mesh and volume mesh controls are invoked to ascertain sufficient mesh resolution in the main interaction zone around air supply diffuser, exhaust and wall boundaries. A total of ≈ 1.06 million computational cells are used for the simulations. The near wall mesh resolution ensures $0.02 < y^+ < 17.06$ for all considered cases. Note that the resolution near ceiling is $0.3 < y^+ < 6.4$ and near floor is $0.08 < y^+ < 6.2$. The boundary conditions are mentioned in Figure 4. Desired mass flow is specified at the diffuser inlet boundary with a constant supply temperature, $T_{in} = 17°C$ and inlet density, $\rho_{in} = 1.216\ kg/m^3$. The exhaust conditions are set as flow outlet with same mass flow value at the inlet with appropriate sign to ensure the global mass conservation. All vertical walls and the floor are set as adiabatic wall boundaries, while a heat loss of 1 W/m^2 is specified on the roof as recommended in the Nordtest method. The internal load in the room is provided via a heat source of 40 W in each wall, giving rise to a total value of 120 W as shown in the Figure 4. This value has been set to mimic the effect of one human occupant. A turbulent intensity of 4% and a length scale of 10% of the inlet diffuser height h are chosen to assign the Dirichlet boundary conditions for κ and ω at the inlet boundary. Zero gradient condition at the outlet and all y^+ wall treatment of the solver is invoked for the remaining no-slip walls regarding these parameters. Converged solutions for all cases are extracted once the residual for mass conservation and energy conservation stabilises $\approx 8 \times 10^{-4}$ and residuals for all remaining equations drops below 4×10^{-5}.

Results and discussion

The flow physics involved in the present ventilation setup is governed by the Archimedes number (analogous to Richardson number) and this can be defined as $Ar = \frac{g\beta}{\rho_{in} c_p} \frac{q_t L}{u_{in}^3 A_s}$ (Brandan (2012)), where c_p is the heat capacity at constant pressure, q_t is the total heat gain in the room, A_s is the diffuser area of the inlet and L is the characteristic length that can be defined as the difference between the room height and height of the diffuser. Eight different test cases are simulated having $Ar = 2, 6, 10, 14, 18, 22, 26$ and 30 as variable parameter leading to the following functional form for any non-dimensional flow variable, $\phi^*(Ar, \vec{x})$. The following analysis is based on the non-dimensional variables: $\rho^* = \frac{\rho}{\rho_{in}}$, $U^* = \frac{u}{u_{in}}$ and $T^* = \frac{(T - T_{in})\ \rho_{in} c_p \dot{V}_{in}}{q_t}$, where $\dot{V}_{in}$ is the volumetric flow rate at the inlet. We first present the CFD solutions for different Ar. Subsequently, the analysis of POD-interpolated solution for $Ar = 15$ is presented.

DV characteristics and CFD snapshots

The Ar is varied essentially setting different inlet air supply velocity with fixed supply T_{in} and ρ_{in} and heat loads as mentioned before. Figure 5 shows the distribution of U^* on a $x - y$ plane at z=0.1m. The typical air flow pattern for low air velocity diffuser in DV configuration involving the acceleration region (near field) and the velocity decay region (far field) can be clearly realised from the U^* contours. With increasing Ar, the maximum value occurs at further upstream (x-coordinate) locations. Evidently, the acceleration zone is larger for low Ar. Figure 6 shows the effective thermal stratification on a $z - x$ plane at the middle of the room ($y = 2.8m$) for all cases which

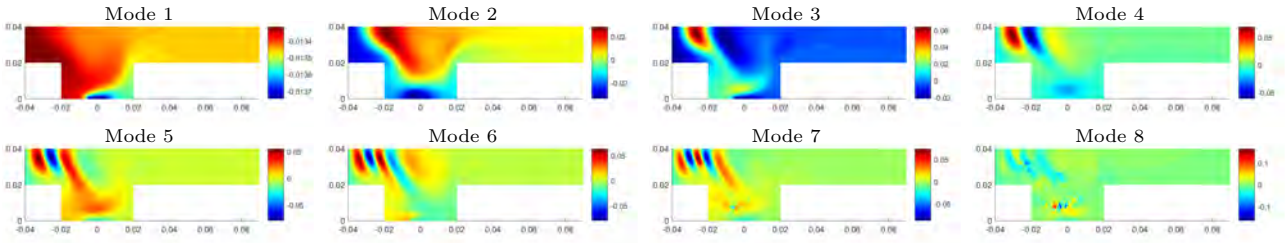

Figure 3: Spatial structures of the POD modes for θ.

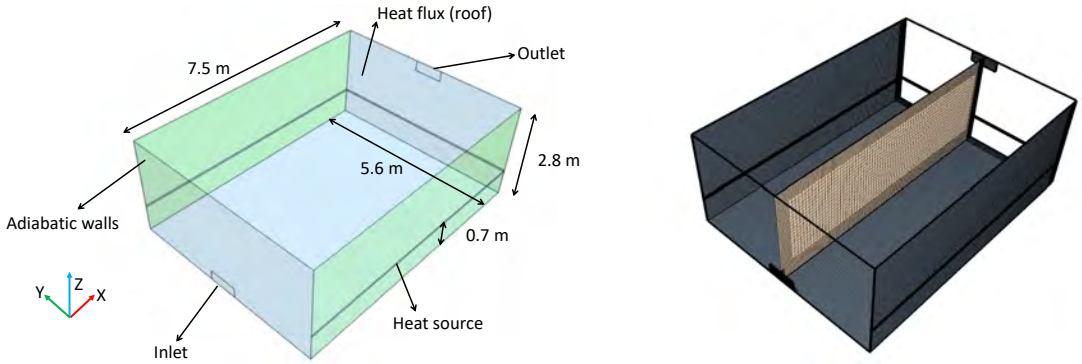

Figure 4: Computational setup of the indoor airflow study, left: domain specification and boundary conditions, right: mesh on some sample planes.

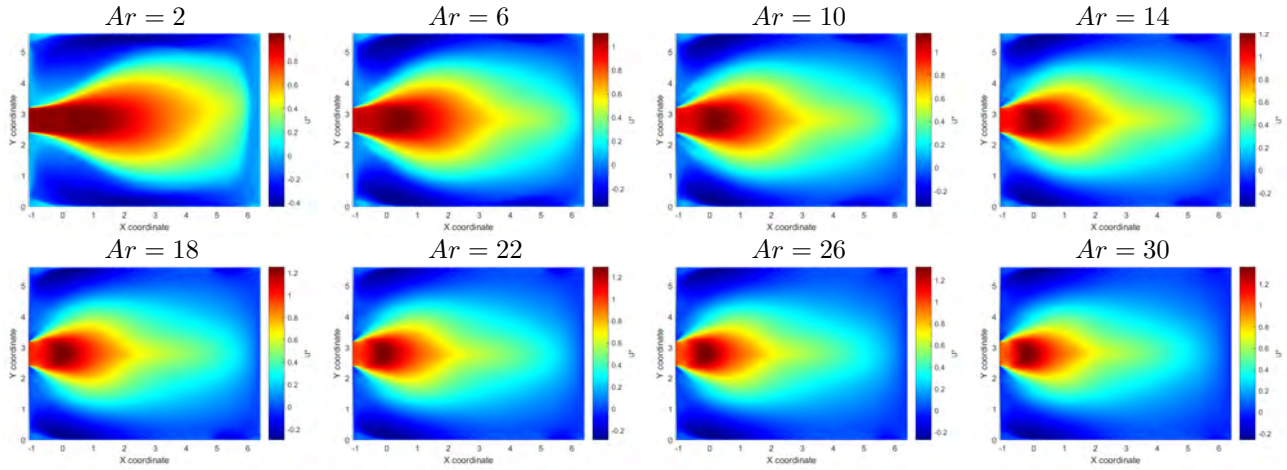

Figure 5: Contours of u-component of the velocity on a horizontal plane at 0.1 m above the floor for different Ar.

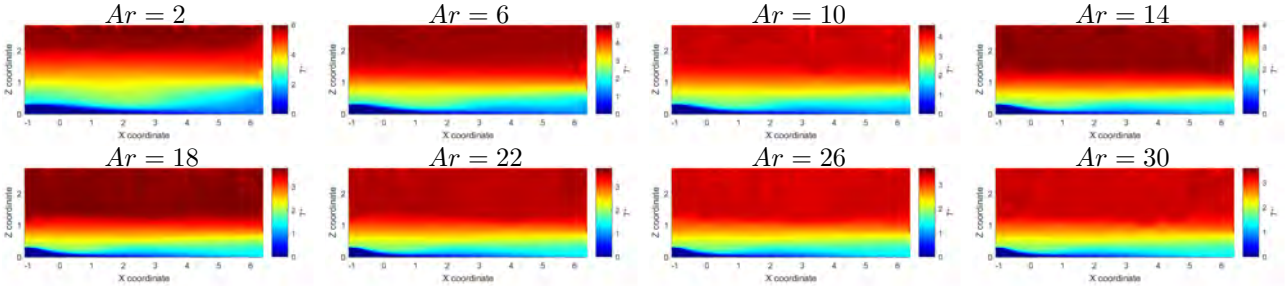

Figure 6: Contours of temperature on a vertical plane in the middle of the room at $y = 2.8m$ for different Ar.

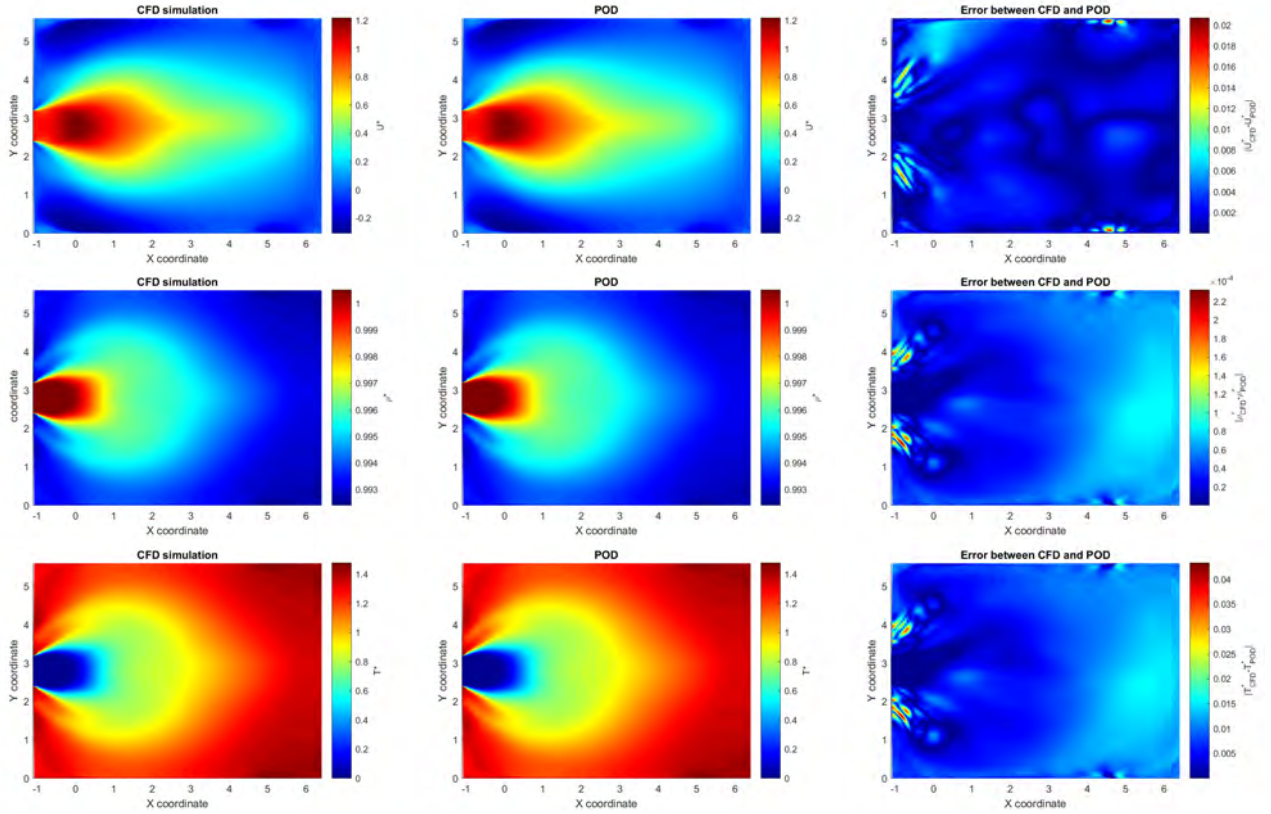

Figure 7: Velocity, density and temperature distributions on horizontal plane at 0.1 m above floor for $Ar = 15$.

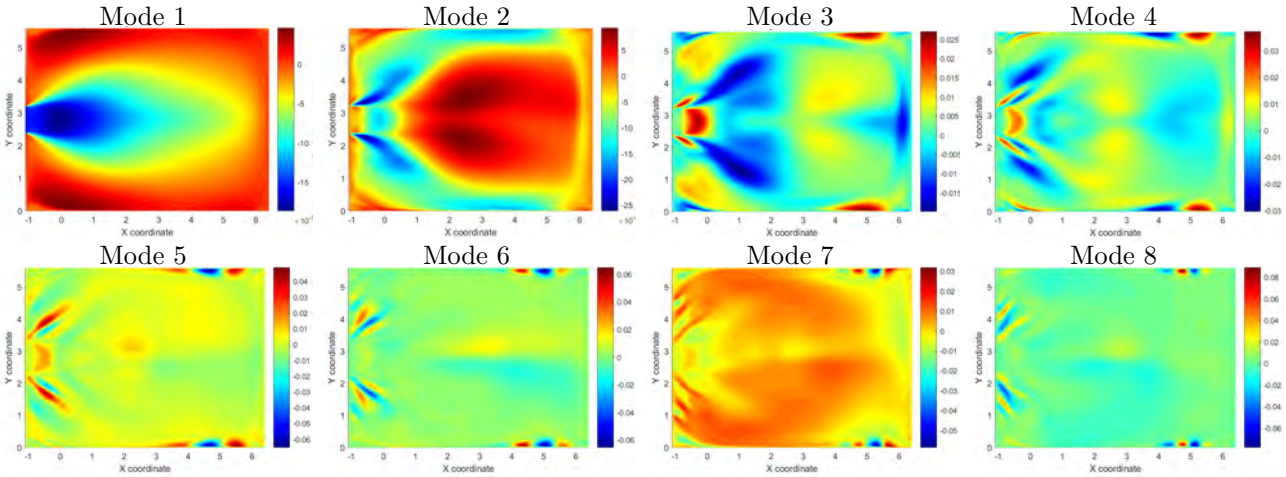

Figure 8: Spatial structures of the POD modes for u-component of the velocity field.

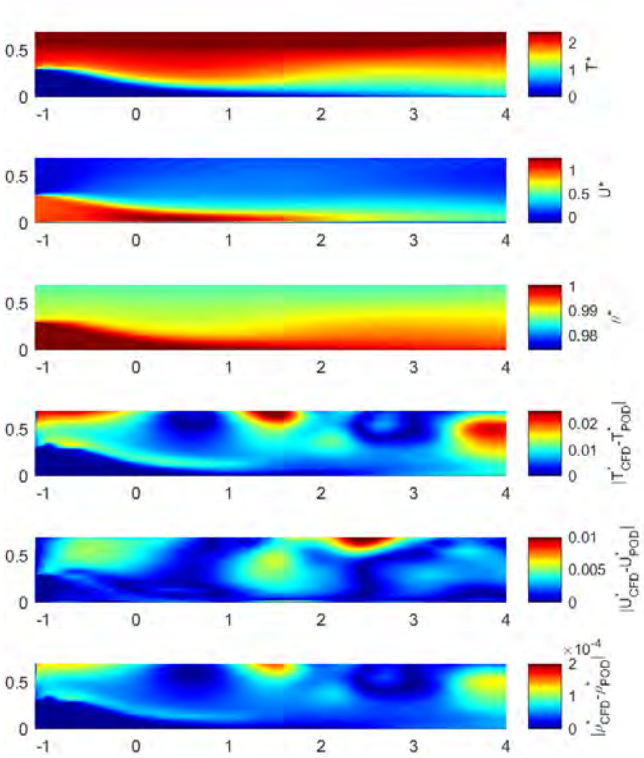

Figure 9: POD predictions and error estimates on a vertical plane at $y = 2.8$ for $Ar = 15$.

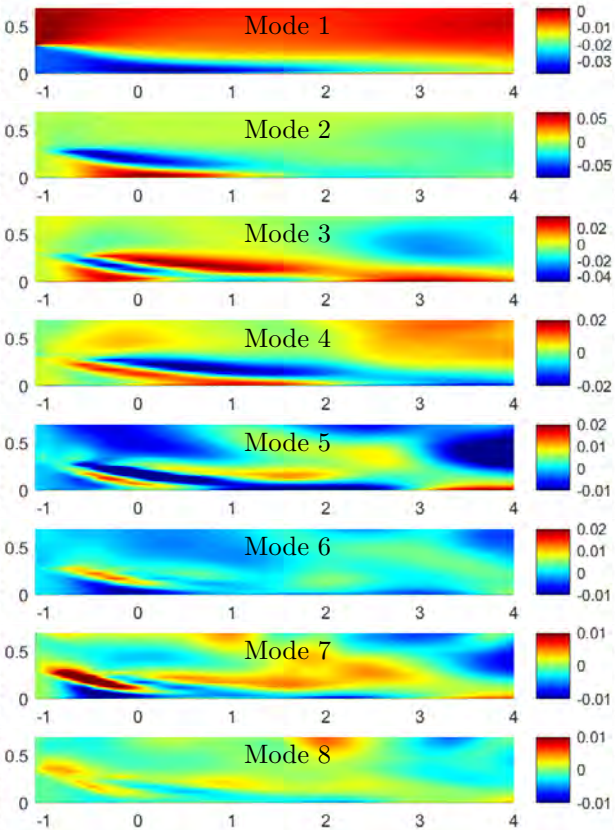

Figure 10: Spatial structures of the POD modes for u-component of the velocity field.

is the key aspect of achieving the good air quality for a DV system.

Analysis of POD-interpolated prediction

The steady state CFD snapshots of 8 different cases are used for the POD. We estimate the flow parameters for $Ar = 15$ via POD-interpolated methodology on two different planes (as discussed above). The predicted contours of U^*, T^* and ρ^* at $x - y$ plane are compared with the actual CFD (see Figure 7) results. It can be seen that the absolute error estimates are sufficiently low and the POD-interpolated predictions are in excellent agreement with the CFD counterpart. The spatial structures of the POD modes of the U^* are shown in Figure 8. Here, we found that the most of the energy contained within the first two POD modes. The energy associated with 8 POD modes are 98.01%, 1.76%, 0.19%, 0.00024%, 10^{-5}%, 10^{-5}%, 10^{-5}%, and 10^{-6}% respectively. A similar trend is observed for the predictions on mid $z - x$ plane (see Figure 9). It is evident that the error estimates for this plane appears relatively higher above the diffuser height levels having relatively coarser mesh. Nevertheless, the errors are sufficiently low in the main interaction zone near and below the diffuser height level. The acceleration and velocity decay regions are predicted very well. The spatial structures of the POD modes are shown in Figure 10. As expected, the first two modes are the most dominant modes among all.

Conclusion

In this work, we have presented a POD-interpolation based methodology in resolving complex indoor airflow patterns and thermal stratification related to a DV system. A 2D thermal convection benchmark problem on a cavity geometry has been solved to verify and validate the overall implementation. The guideline of the Nordtest method is adopted to build the case studies associate with a DV configuration for a standard room. Steady-state CFD snapshots with a varying Archimedes number are used to estimate the dominant POD coefficients/modal amplitudes and POD modes. The flow field variables are decomposed in terms of Archimedes number dependent POD coefficients and associated space dependent POD bases. A cubic spline interpolation of the POD coefficients is used to predict the solution for intermediate value of Archimedes number. The analysis reveals that for the u-component of the velocity field the first two POD modes are the most dominant modes accounting the associated energy $\approx 99.8\%$.

The present study clearly shows the capability of CFD snapshot based POD-interpolated fast and reliable predictions of DV configuration involving a wall mounted linear air terminal device. A future study with the different types of air terminal devices could be undertaken and this fast prediction approach is potentially advantageous to carry out further parametric variations without performing a large number

of physical experiments and validate existing semi-empirical models of DV systems.

Acknowledgment

The authors greatly acknowledge the commercial computer program StarCCM+, used in this study. The CFD results are obtained by the licensed version 2019.2 (Build 14.04.011-R8) on a stand alone desktop at OsloMet—Oslo Metropolitan University.

References

Aminossadati, S. M. and B. Ghasemi (2009). A numerical study of mixed convection in a horizontal channel with a discrete heat source in an open cavity. *European Journal of Mechanics-B/Fluids 28*(4), 590–598.

Brandan, M. (2012). *Study of airflow and thermal stratification in naturally ventilated rooms*. Ph. D. thesis, Massachusetts Institute of Technology.

Brunton, S. L., B. R. Noack, and P. Koumoutsakos (2020). Machine learning for fluid mechanics. *Annual Review of Fluid Mechanics 52*, 477–508.

Cao, G., H. Awbi, R. Yao, Y. Fan, K. Sirén, R. Kosonen, and J. J. Zhang (2014). A review of the performance of different ventilation and airflow distribution systems in buildings. *Building and environment 73*, 171–186.

Causone, F., F. Baldin, B. W. Olesen, and S. P. Corgnati (2010). Floor heating and cooling combined with displacement ventilation: Possibilities and limitations. *Energy and Buildings 42*(12), 2338–2352.

Cehlin, M. and B. Moshfegh (2010). Numerical modeling of a complex diffuser in a room with displacement ventilation. *Building and Environment 45*(10), 2240–2252.

Choi, N., T. Yamanaka, K. Sagara, Y. Momoi, and T. Suzuki (2019). Displacement ventilation with radiant panel for hospital wards: Measurement and prediction of the temperature and contaminant concentration profiles. *Building and Environment 160*, 106197.

Davidson, L. (1989). Ventilation by displacement in a three-dimensional room—a numerical study. *Building and environment 24*(4), 363–372.

Elhadidi, B. and H. E. Khalifa (2005). Application of proper orthogonal decomposition to indoor airflows. *Ashrae Transactions 111*(1).

Gilani, S., H. Montazeri, and B. Blocken (2016). Cfd simulation of stratified indoor environment in displacement ventilation: Validation and sensitivity analysis. *Building and Environment 95*, 299–313.

Javad, K. and G. Navid (2019). Thermal comfort investigation of stratified indoor environment in displacement ventilation: Climate-adaptive building with smart windows. *Sustainable Cities and Society 46*, 101354.

Khalifa, H. E., B. Elhadidi, and J. F. Dannenhoffer III (2007). Efficient coupling of multizone and cfd indoor flow models through proper orthogonal decomposition. *ASHRAE Transactions 113*(2).

Li, Y., M. Sandberg, and L. Fuchs (1992). Vertical temperature profiles in rooms ventilated by displacement: Full-scale measurement and nodal modelling. *Indoor Air 2*(4), 225–243.

Magnier, L., R. Zmeureanu, and D. Derome (2012). Experimental assessment of the velocity and temperature distribution in an indoor displacement ventilation jet. *Building and Environment 47*, 150–160.

Meyer, K. E., J. M. Pedersen, and O. Özcan (2007). A turbulent jet in crossflow analysed with proper orthogonal decomposition. *Journal of Fluid Mechanics 583*, 199–227.

Nielsen, P. V. (1988). Displacement ventilation in a room with low-level diffusers.

Nielsen, P. V. (2000). Velocity distribution in a room ventilated by displacement ventilation and wall-mounted air terminal devices. *Energy and Buildings 31*(3), 179–187.

Nordtest (2003). Air terminal devices: Aerodynamic testing and rating at low velocity (NT VVS 083).

Selimefendigil, F. (2013). Numerical analysis and pod based interpolation of mixed convection heat transfer in horizontal channel with cavity heated from below. *Engineering Applications of Computational Fluid Mechanics 7*(2), 261–271.

Sirovich, L. and M. Kirby (1987). Low-dimensional procedure for the characterization of human faces. *Josa a 4*(3), 519–524.

Wei, G., B. Chen, D. Lai, and Q. Chen (2020). An improved displacement ventilation system for a machining plant. *Atmospheric Environment*, 117419.

Yuan, X., Q. Chen, and L. R. Glicksman (1998). A critical review of displacement ventilation. *ASHRAE Transactions-American Society of Heating Refrigerating Airconditioning Engin 104*(1), 78–90.